Conference Proceedings

Solar World Congress 2015
Daegu, Korea, 08 – 12 November 2015

CONCENTRATED FLUX MEASUREMENT APPARATUS FOR AN ASYMMETRICAL PARABOLIC TROUGH SOLAR CONCENTRATOR

Matteo Bortolato[1, 2], Simone Dugaria[1] and Davide Del Col[1]

[1] Department of Industrial Engineering (DII), University of Padova, Padova, Italy

[2] Interdepartmental Centre "Giorgio Levi Cases" for Energy Economics and Technology, University of Padova, Padova, Italy

Abstract

In this work, the optical performance of an asymmetrical small parabolic trough solar concentrator is experimentally characterized by adopting a direct method to define the solar flux map on the focal region. Due to the particular geometry of the optical system, the optimal plane of concentration is 45° tilted with respect to the plane containing the focal line and the vertex line. A water cooled heat flux microsensor installed on a two-axes linear handling system is used to measure the concentrated solar flux along the optimal concentration plane of the present optical system. The collected data are interpolated to obtain the flux distribution and to determine the width of the solar image over the focal line. These results together with the values of the direct normal irradiance collected during the tests and the nominal reflectance of the parabolic mirrors allow the evaluation of the intercept factor for different areas included in the concentration region.

Keywords: *solar flux mapping; heat flux microsensor; optical performance; parabolic trough, intercept factor*

1. Introduction

A parabolic trough solar collector consists of an optical system, named concentrator, that reflects the beam radiation onto a focal region, where a receiver is installed to convert the solar radiation into heat or electric energy. In order to work efficiently throughout the day, the system must be equipped with a tracking system to maintain the sun vector on the plane normal to the aperture area and containing the focal line. The ratio between the aperture area of the concentrator and the receiver area is defined as the geometrical concentration ratio and it qualitatively provides the operating temperature range of a concentrating collector. In ideal optics, parallel rays normally incident on the aperture area of a parabolic trough are concentrated along a focal line. In real applications, there is a concentration region around the focal line, whose width depends on the sunshape and on the total optical error. The sunshape represents the brightness intensity distribution across the finite angular size of the sun disc and the circumsolar aureole. The total optical error includes the shape and specular reflectance errors of the parabolic mirrors, the tracking error and the imperfect positioning and alignment of the receiver.

Experimental measurements and the development of reliable models implemented in Monte Carlo ray tracing tools become pivotal for the design and improvement of concentrating solar collectors. In the case of a parabolic trough collector, periodical monitoring the concentrated solar flux and its distribution is recommended to assess the accuracy of the tracking system, the durability of the mirror reflectance and the stiffness of the structure over time. Furthermore, the geometry and the configuration of the receiver should be designed according to the width of the concentration region and the solar flux distribution in order to optimize the performance. Once the solar map has been measured, given the aperture width of the receiver, one can calculate the intercept factor, that is the fraction of the beam radiation reflected by the mirrors and

doi:10.18086/swc.2015.10.22 Available at http://proceedings.ises.org

reaching the receiver. To ensure acceptable performance of the solar concentrating collector, the intercept factor should be higher than 90%.

The arrangement of the solar cells in a photovoltaic receiver and, if necessary, a secondary optics must be design considering that the non uniformity of the incident flux is expected to cause hot spots, current mismatch and to penalize the efficiency (Baig et al., 2013). On the other hand, in solar thermal collectors, the non uniform distribution of the concentrated solar flux on the external surface of the absorber can lead to perimetral temperature gradients. This is associated to differential thermal expansions that cause thermal stresses, whose effect can be very serious in some working conditions (Khanna et al., 2013, 2014, 2015, Eck et al., 2007). In common practice, a high mass flow rate is pumped in order to achieve a turbulent flow condition inside the tubular absorber- This approach is generally adopted in solar power plants but cannot be applied in small medium temperature concentrating collectors, especially for direct steam generation, where a certain flexibility of operation is required to maximize the working hours per day under stable conditions. The solar flux mapping is of great importance in the design of receiver with enhancement heat transfer.

In general, the measurement of the concentrated solar flux on the focal region can be performed through different techniques that can be classified as direct, indirect and measurement-supported simulation methods.

Direct methods refer to the use of a flux sensor, whose response can be directly associated with the concentrated flux. In order to get a fine spatial resolution of the measured concentrated solar flux, these sensors should have a small aperture and should be either distributed in the focal region or installed in handling systems (Röger et al., 2014). Both the techniques require the interpolation of the experimental data collected in specific points of the concentration region to get the solar flux map. In the former, several sensors are needed to obtain results with low uncertainty, but this entails that the measurement system has a very high investment cost. Furthermore, the spatial resolution may only be modest. In the latter solution, a handling system should be designed according to the geometry of the investigated concentrator; this solution allows to scan quickly the focal region and to collect much more experimental points as compared to the case of stationary and distributed sensors, thus increasing the accuracy of the results. The most common sensors employed in concentrating collectors analysis are radiometers and calorimeters (Ballestrín et al., 2012).

Radiometers deliver an electrical response that may be a voltage coming from a differential temperature sensor such as a thermocouple for the Gardon radiometer or a thermopile for the more recent heat flux microsensors (HFMs) or a current generated by a photodetector. Heat flux microsensors have been used by Ballestrin (2002) to investigate the concentrated solar flux distribution on a central volumetric receiver of a heliostat field at the Plataforma Solar de Almeria. Ferriere and Rivoire (2002) and Parretta et al. (2007) designed and realized two different radiometers arranging a photodetector respectively inside a single integrating sphere and two integrating spheres optically interconnected. Fernández-Reche et al. (2008) presented a comparative test performed in a solar furnace measuring concentrated solar flux using both a Gardon radiometer and a GaAs photovoltaic cell as photodetector. Riffelmann et al. (2006) developed the parabolic trough flux scanner (PARASCAN) to detect the solar flux on the tubular receiver of parabolic trough collectors having an aperture width of 5.76 m. The measurement system consists of two arrays of 96 photodiodes each, placed behind translucent Lambertian targets. The first array is arranged in front of the receiver tube, to detect the beam irradiance reflected by the mirrors towards the concentration region, while the second array is located behind the receiver, to measure the optical losses. The two arrays are fixed on a sliding carriage moved by a remote control. From the integrated values collected by the first and the second array, the intercept factor of the parabolic concentrator can be calculated.

When using a calorimeter mounted in the focal region of a concentrator, the solar flux can be derived from a thermal balance between the radiant power incident on the device aperture and the heat flow rate transmitted to a cooling fluid flowing through the sensor. Pérez-Rábago et al. (2006) and Estrada et al. (2007) employed calorimeters to measure the solar flux in point focus concentrators.

In indirect methods, digital cameras (CMOS cameras or, more often, CCD cameras) equipped with appropriate filters and zoom lenses are used to capture one or more images that can be related to the solar flux distribution after processing. The captured images are in gray-scale map, so they can only give qualitative information. In order to correlate the gray-scale value of each pixel to a physical irradiant flux value, the system must be calibrated in situ. If accurately implemented and calibrated, indirect methods provide very high spatial resolution , high reliability and short measurement time.

In most cases, the digital cameras register the solar radiation reflected off a target which exhibits a diffuse reflectance very close to ideal Lambertian reflectance (camera-target method). This means that, whatever the angle of observation, the target surface appears equally bright. Ballestrín and Monterreal (2004) evaluated the concentrated solar flux on a central receiver of a heliostat fields by capturing images with a CCD camera on a moving uncooled Lambertian target. This target swings in front of the receiver aperture area and intercepts the reflected solar beam radiation in a measurement plane. Moving the target is necessary in high concentration ratio systems, where the concentrated flux may overheat and damage it. Two water-cooled Gardon radiometers placed very close to the receiver aperture are used to calibrate the CCD camera. Riffelmann et al. (2006) implemented the calibrated CCD camera-target method for flux mapping on the focal region of a parabolic trough concentrating solar collector. The Lambertian target has a notch which allows to enclose the tubular receiver and it can be moved through a telescopic arms along the focal region. On the target, higher and lower concentration areas as well as solar rays missing the absorber tube can be observed. After image processing, an approximate value of the local intercept factor can be calculated.

A new method, that has been applied to few receivers so far (Ho and Khalsa, 2012, Röger et al., 2014), regards the use of a digital camera only, without target, applied to external receivers. It is related to many sources of error that should be carefully taken into account. First, as the assumption of a perfectly diffusing material of the receiver is definitely not exact, its real reflectance should be characterized using a gonioreflectometer. Secondly, the receiver is provided with a selective coating with a high absorbance in the wavelength range of the solar spectrum and has a surface temperature much higher than the ambient air temperature. Hence, a special filter that can cut off thermal radiation emitted by the receiver in the infrared range should be adopted. Finally, the use of different filters during calibration procedure and during tests may entails error due to the difference between the actual attenuation factors and the manufacturers' specifications. Total errors associated to this method can be up to 20% - 40%, mainly because of large uncertainty in receiver reflectance and in filters' attenuation factors.

Lüpfert et al. (2008) presented a second version of PARASCAN to evaluate the flux distribution on the focal region of a parabolic trough with great accuracy. Fiber optics are arranged instead of photodiodes, behind the translucent Lambertian targets of the two parts of the moving measurement system. Each sensor part is composed by 12 segments where 16 optical fibers are mounted at distances of 2.5 mm., giving a very high spatial resolution. The optical fibers transmit the beam radiation concentrated on the focal region to a CCD camera equipped with neutral density filters, out of the hot region. A direct calibration of the system under natural sunlight is possible. From the measured flux maps, intercept factor have been calculated with an experimental uncertainty of ± 1%.

The last class of methods involves the use of ray tracing codes, which have proved to be powerful tools to model many types of solar concentrating collector and to obtain prediction of the solar flux on any surface. Nevertheless, the accuracy of the results depends on the quality of the input parameters: shape, tracking and receiver positioning errors, optical defects, optical properties of the materials and atmospheric conditions. Furthermore, the results should be validated against merely experimental measurements, in which, in this case, a high resolution and an extreme complexity is not required. Schiricke et al. (2009) developed an optical model of a parabolic trough solar concentrator by implementing in a Monte Carlo ray tracing software the photogrammetrically measured geometry of the collector, the nominal optical properties of the materials, the incidence angle of the solar rays on the aperture area, the measured values of direct normal irradiance and assuming a typical clear-sky sunshape. The model has been validated by comparing the simulated intercept factors and the flux map to those measured with an indirect method. It proved to be very accurate and reliable, hence it can be use to study the effect of different combinations of parameters on the collector performance.

In this work, a direct method based on the use of a radiometer mounted on a handling system is used to measure the solar flux map on the concentration region of an asymmetrical parabolic trough concentrator that has been designed for installing receivers with flat absorbers.

2. Experimental apparatus

The small parabolic trough concentrator considered in this work is asymmetrical since the reflective optics extends from the vertex line to the mirror rim (Fig. 1). It has been installed at the Solar Energy Conversion Lab of the Industrial Engineering Department, University of Padova. The present concentrator exhibits an aperture width of 2.9 m, a rim angle of 78°, a focal length of 1.81 m and a trough length of 2.4 m, resulting in an aperture area equal to 6.857 m^2. The reflecting optical system is made up by four back silvered glass facets arranged in two rows, which have a nominal reflectance of 96%, as provided by the manufacturer. Due to the small dimensions of the prototype, it is equipped with a two-axes solar tracking system to have the beam radiation normal to the aperture area without any cosine loss. The motion is governed by a solar algorithm when approaching the sun and by a sun sensor to achieve the best alignment. The particular geometry of the present parabolic trough concentrator is suitable to be coupled with a receiver provided with a flat geometry absorber. As an example, the receiver may be similar to some trapezoidal cavity receivers generally mounted on linear Fresnel solar collectors. In order to minimize the incidence angle of the concentrated beams on a flat receiver, the optimal concentration plane of this system is 45° tilted with respect to the plane containing the focal line and the vertex line.

.

Fig. 1: Prototype of the asymmetrical parabolic trough linear solar concentrator and solar flux map measuring system installed at the Solar Energy Conversion Lab of the University of Padova.

The solar flux mapping system has been designed so that the measuring plane corresponds to the optimal concentration plane. A water-cooled heat flux microsensor is mounted on a two axes (x, z) semi-automatic linear handling system. The horizontal axis (x-axis) is parallel to the trough length and the second axis (z-axis) lies on the width of the concentration region on the measuring plane. As declared by the manufacturer, heat flux microsensors have a very fast response time of 300 μs when the face is provided with a high absorptance black coating, as usual for radiant flux measurement in concentrating solar collectors. Water cooling of the sensor is necessary for applications requiring a continuous monitoring of the concentrated flux and to reduce the influence of the ambient conditions on the measurement accuracy. In fact, if the average temperature of the cooling fluid (distilled water) passing through the sensor is maintained close to the ambient air temperature, the effect of convective heat losses on the measurement of the concentrated flux can be neglected.

The horizontal x-axis is provided with a sliding carriage that can be fixed at several repeatable position along the trough length by appropriate blocking elements. On the sliding carriage, an electrical linear actuator is mounted and it allows the movement of the sensor along the z-axis to scan the concentration region. the actuator has a stroke of 150 mm, a variable speed from 0.001 m s^{-1} to 2 m s^{-1} and a maximum positioning repeatability of 0.1 mm. On the top of the actuator, an aluminum structure supports the sensor and allows fine adjustments to make the optimal concentration plane and the measuring plane match (Fig. 2). The handling system has been mounted so that the heat flux microsensor moves on the optimal concentrating plane (Fig. 3).

Fig. 2: Electric linear actuator mounted on the sliding carriage of the x-axis and water-cooled heat flux microsensor arranged on a supporting structure.

Fig. 3: Position of the heat flux microsensor when the electric linear actuator is completely down (position 0).

The laboratory includes a first class pyrheliometer mounted on a high precision solar tracker that is used to measure the direct normal irradiance (DNI). A datalogger registers the electrical signals associated to the position of the actuator, the measured solar flux, the temperature of the heat flux microsensor's face and the direct normal irradiance with a sampling rate of 0.2 s and the collected data are reduced in Matlab® environment.

3. Experimental technique and data reduction

Before every experimental test, the reflecting facets of the parabolic trough concentrator, the sun sensor and the pyrheliometer have been cleaned. The solar flux map has been experimentally characterized on a trough length of 1200 mm along the x-axis, corresponding to a single row of parabolic mirrors. Along the investigated trough length, ten blocking elements have been arranged at a distance of 120 mm. Concentrated solar flux measurements have been performed according to the following procedure. The electrical linear actuator is brought at the first station in its zero position, in which the heat flux microsensor is 65 mm under the ideal focal line of the concentrator. The zero position of the actuator corresponds to the origin of the z-axis. Then, the working cycle of the actuator is started. It consists of a slow rise for collecting the experimental data and a quick descent to return in the zero position before being moved to the next position along the x-axis. At the end of the slow rise phase, the sensor is 65 mm above the ideal focal line, thus the investigated width on the concentration region is of 130 mm, centered on the ideal focal line. During each test, four values are registered by the data acquisition system: the position of the sensor, given by the electrical output signal of the actuator's encoder, the heat flux and the temperature signal from the heat flux microsensor and the direct normal irradiance measured by the pyrheliometer. The series of data collected during a tests are considered for data reduction in a Matlab® environment if the variations of the direct normal irradiance is within the experimental uncertainty of the pyrheliometer (± 2.5 % of the average value, with a level of confidence of 95.45 %). The number of collected data for concentrated solar flux depends on the number of measuring position along the x-axis, the actuator's speed along the z-axis and the sampling rate allowable by the data acquisition system: the higher the number of experimental data the more accurate the resulting solar flux map. The heat flux microsensor is cooled by a flow of 0.017 kg s^{-1} of distilled water. The temperature of the cooling fluid at the inlet of the sensor is kept constant by dissipating the heat flow rate coming from the concentrated solar radiation to the ground water. Several tests have been conducted consecutively, in order to assess the repeatability of the proposed measuring technique under very similar test conditions.

The face of the sensor is coated with Pyromark 1200, a high temperature paint which has an emittance of 95 % as declared by the calibration report. According to the study by (Song et al., 2014), the total infrared spectral emittance of this coating is higher than 93% in the wavelength range between 3 μm and 14 μm. Therefore, unlike other coatings (Ballestrín et al., 2003), there is no need to introduce corrective dimensionless factors to account for the differences between the solar irradiance spectrum and the irradiance spectrum of the black body employed for the calibration of heat flux microsensors.

The procedure described in the work by Ballestrin (2002) has been adopted to evaluate the optical performance of the present asymmetrical concentrator. In order to define accurately the solar flux map and to calculate the incident power on an area of the concentration region, an interpolation of the experimental data has been performed. The interpolant should be able to predict well local trends, therefore the spline interpolants have been considered. Differently from the study by Ballestrin (2002), where an aiming strategy of 25 heliostats was set up to obtain a uniform flux distribution on the central receiver, in the present parabolic trough concentrator, a strongly non uniform flux distribution is expected. As a consequence, the spatial resolution to interpolate should be quite small to get a more accurate estimation of the incident power on an area of interest included in the focal region. In fact, the incident power is calculated by a numerical integration of the solar flux distribution, dividing the area of interest into *n* equal rectangular elements and using the tiled method, according to eq.1:

$$P_{inc} = \frac{A_{cr}}{n} \sum_{i=1}^{n} q_i'' \qquad \text{(eq. 1)}$$

where *n* is the number of data in the area of interest, A_{rc} is the surface of the area of interest and q''_i is the i-th value of solar flux. Unfortunately, the spline interpolants do not allow the estimation of the uncertainty on predicted concentrated solar flux values. Therefore, in order to assess if the number of collected data is sufficient for a good definition of the solar flux map, different interpolants (linear, cubic and biharmonic) have been considered and the results of the numerical integration have been compared. If the obtained value of the power incident on an area of the concentration region does not change significantly when varying the interpolant, the accuracy in the solar flux map definition can be considered satisfactory. Once the incident power onto an area of interest has been calculated, the associated intercept factor γ can be determined as follows (eq. 2):

$$\gamma = \frac{P_{inc}}{\mathrm{DNI}\, A_{ap}\, \rho_{mir}} \qquad \text{(eq. 2)}$$

where DNI is the average value of the direct normal irradiance during the considered test run, A_{ap} is the aperture area of the row of mirrors and ρ_{mir} is the nominal reflectance of the mirrors, provided by the manufacturer.

The experimental uncertainty of the calculated power P_{inc} is derived from the combination of the integration uncertainty, the interpolation uncertainty and the uncertainties related to the handling system positioning and movement. The interpolation uncertainty has been computed as in the work by Ballestrin (2002). The interpolation uncertainty can be neglected because the chosen interpolant shall not affect the results. Furthermore, the geometry of the present asymmetrical parabolic trough concentrator allows to check that the measuring plane matches the optimal concentration plane. Finally, the uncertainty of the intercept factor has been calculated applying the law of propagation of uncertainty for uncorrelated inputs (Joint Committee for Guides in Metrology, 2008) and neglecting the uncertainty of the nominal reflectance of the parabolic mirrors.

4. Results and discussion

Experimental measurements of the solar flux distribution on the concentration region of the asymmetrical parabolic trough concentrator have been performed consecutively during a clear sky day. The dimensions of the measuring area, which is the area scanned by the heat flux microsensor, are given by the actual stroke of the electrical linear actuator along the z-axis (130 ± 1 mm) and by the distance between the first and the last of the blocking elements along the x-axis (1082 ± 1 mm). During the presented test runs, the direct normal irradiance was around 890 W m^{-2} and the ambient air temperature was around 23°C. The water cooling of the microsensors allow to keep the temperature of its face between 19°C and 23°C during each scan of the concentration region. The speed of the electric linear actuator was set equal to 0.005 m s^{-1} in the rise phase and equal to 0.1 m s^{-1} in the descent phase. Measured data were sampled with a scan interval of 0.2 s. The resulting spatial resolution along the width of the concentration region is 1 mm and 1300 concentrated solar flux data were collected during each test. The spline interpolation has been executed over a grid with a spatial resolution of 1 mm x 1 mm, giving a set of 141873 data on the whole measuring area. A finer spacing does not entail significant variations in the calculation of the incident power on an area included in the measuring area, whatever its width.

Fig. 4 reports the 3D solar flux distribution obtained after interpolating the experimental data (blue dots) collected in a single test run through the biharmonic spline method. The origin of the z-axis corresponds to the zero position of the encoder integrated in the electrical linear actuator, while the origin of the x-axis corresponds to the projection of the external rim of the mirrors on the ideal focal line. The equation of the ideal focal line is z = 65 mm. For the sake of clarity, the solar map has been presented with a spatial resolution lower than that adopted for the calculation of the concentrated power on an area of interest included in the measuring area.

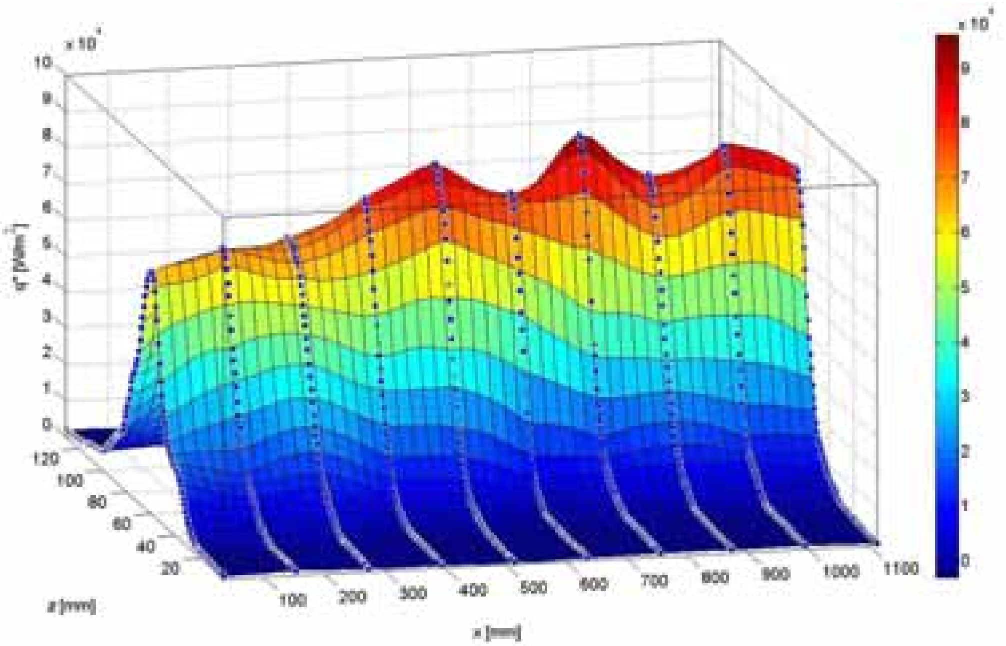

Fig. 4: Three-dimensional solar map on the measuring area defined during the experimental study of the optical performance of the asymmetrical parabolic trough installed at the University of Padova. The reported surface has been obtained after interpolating the experimental data through the biharmonic spline method.

As expected, the solar flux distribution is strongly non uniform along the width of the concentration region (z-axis). Nevertheless, there are significant variations of the solar flux even along the x-axis: the external rim of the mirrors in the considered row appears to be less efficient in concentrating the solar beam. In fact, differently from the rest of the measuring area, the solar flux is below 80 kW m^{-2} on the first 300 mm of the investigated trough length. The maximum peak value of the measured concentrated solar flux is 96250 W m^{-2} at x = 750 mm, while the minimum peak value of 66900 W m^{-2} has been detected at the very beginning of the trough length (x = 33 mm). The isoflux contour plot related to the same test run is reported in Fig. 5: one can notice that the maximum width of the concentration region is of 100 mm and it centered on the focal line. On the central part of the mirrors composing the investigated row, the concentration of the solar beams is performed on a tighter width. According to the previous considerations, the calculation of the concentrated power and the determination of the intercept factor has been performed considering a trough length equal to the measuring area length (1082 mm) and two different widths: 100 mm and 70 mm.

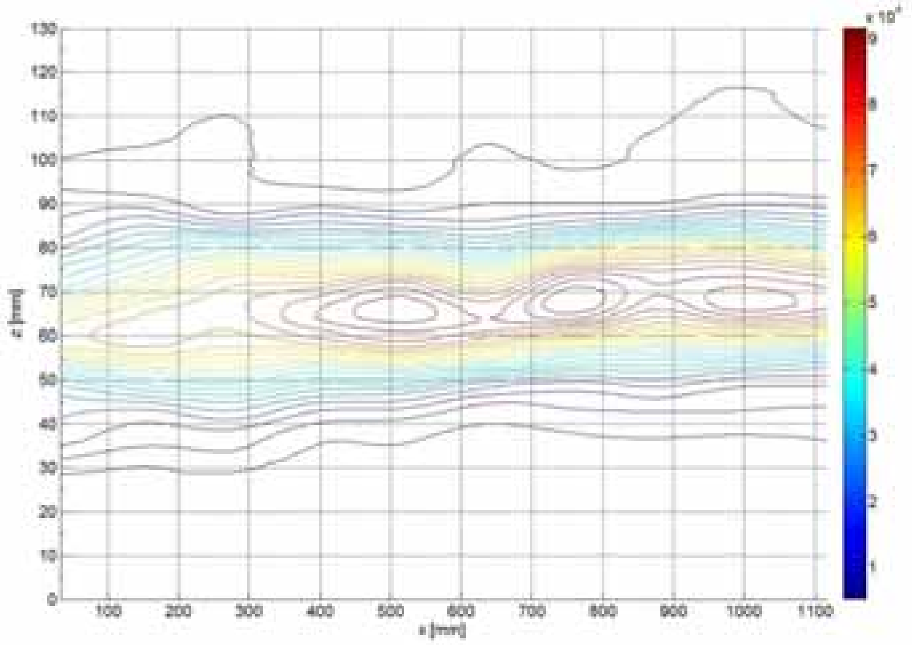

Fig. 5: Concentrated solar isoflux contour plot on the measuring area defined during the experimental study of the optical performance of the asymmetrical parabolic trough installed at the University of Padova.

Considering the solar flux map on the measuring area of Fig. 4, which has been obtained under a direct normal irradiance of 887 W m^{-2}, the concentrated power incident on an area of interest having a width of 100 mm is equal to 2705 W, while it results equal to 2604 W when the width is 70 mm. The variation of the concentrated power values is within ± 0.2 % when different spline interpolants are employed, which demonstrates that the number of experimental data collected during a single test run is high enough to get an accurate definition of the concentrated solar flux distribution on the measuring area. The experimental uncertainty of the concentrated power is between 4% and 5 % and it slightly increases when the width of the area of interest decreases. Considering these results and the nominal reflectance of the mirrors, the intercept factor is of 100% for a 100 mm width, which is consistent with the contour plot of Fig. 5, and it is of 97 % for a width of 70 mm. The shapes of the 3D surface resulting from the different test runs as well as the concentrated powers and the intercept factors on an area of interest do not vary significantly. This proves the repeatability and the reliability of the proposed experimental technique.

5. Conclusions

The solar flux map on the focal region of a prototype of an asymmetrical parabolic trough concentrator has been experimentally determined at the Solar Energy Conversion Laboratory, at the University of Padova. The solar mapping system is composed by a two-axes semi-automatic linear handling system and by a heat flux microsensor. The actual measuring area is 1082 mm x 130 mm, thus it includes a single row of mirrors of the present concentrator. During a single test run, data of the sensor position, concentrated solar flux, temperature of the sensor face and direct normal irradiance are acquired at scan interval with 0.2 s. To define the solar flux map, the collected data have been interpolated by a spline interpolant over a grid with a spatial resolution of 1 mm x 1 mm. The obtained 3D surface for the concentrated solar flux distribution has been numerically integrated to calculate the concentrated power as a function of the width taken in the measuring area. Considering the nominal reflectance of the mirrors and the measured values of the direct normal irradiance, the intercept factor can be calculated for a certain area included in the concentration region.

According to the results, the solar flux distribution is strongly non uniform along the width of the concentration region and there are significant variations of the concentrated solar flux even along the trough length. In particular, the external part of the mirrors provide lower peak flux values near the focal line. The maximum width of the concentration region is 100 mm, whose corresponds a intercept factor of 100%. When considering a width of 70 mm, the intercept factors decreases to 97 %. The calculated value of the intercept factor varies within ± 0.2 % when different spline interpolants are considered and this entails that the number of collected data is high enough to get an accurate definition of the solar flux map. Several tests have been performed consecutively under the same test conditions and the variation of the results is negligible, proving the reliability and the repeatability of the proposed technique.

References

Baig, H., Sarmah, N., Heasman, K.C., Mallick, T.K., 2013. Numerical modelling and experimental validation of a low concentrating photovoltaic system. Solar Energy Mater. Solar Cells 113, 201-219.

Ballestrín, J., Burgess, G., Cumpston, J., 2012. 18 - Heat flux and temperature measurement technologies for concentrating solar power (CSP), in Lovegrove, K., Stein, W. (Eds.), Concentrating Solar Power Technology. Woodhead Publishing, pp. 577-e4.

Ballestrín, J., Monterreal, R., 2004. Hybrid heat flux measurement system for solar central receiver evaluation. Energy 29, 915-924.

Ballestrin, J., 2002. A non-water-cooled heat flux measurement system under concentrated solar radiation conditions. Solar Energy 73, 159-168.

Ballestrín, J., Ulmer, S., Morales, A., Barnes, A., Langley, L.W., Rodríguez, M., 2003. Systematic error in the measurement of very high solar irradiance. Solar Energy Mater. Solar Cells 80, 375-381.

Eck, M., Uhlig, R., Mertins, M., Häberle, A., Lerchenmüller, H., 2007. Thermal Load of Direct Steam-Generating Absorber Tubes with Large Diameter in Horizontal Linear Fresnel Collectors. Heat Transfer Eng. 28, 42-48.

Estrada, C.A., Jaramillo, O.A., Acosta, R., Arancibia-Bulnes, C.A., 2007. Heat transfer analysis in a calorimeter for concentrated solar radiation measurements. Solar Energy 81, 1306-1313.

Fernández-Reche, J., Sánchez, M., Alonso, M., Cañadas, I., Chenlo, F., Rodríguez, J., Ballestrín, J., 2008. Concentrating PV: An Alternative to Calorimeters for Measuring High Solar Flux Densities. Journal of Solar Energy Engineering 130, 044502-044502.

Ferriere, A., Rivoire, B., 2002. An instrument for measuring concentrated solar-radiation: a photo-sensor interfaced with an integrating sphere. Solar Energy 72, 187-193.

Ho, C.K., Khalsa, S.S., 2012. A Photographic Flux Mapping Method for Concentrating Solar Collectors and Receivers. Journal of Solar Energy Engineering 134, 041004-041004.

Joint Committee for Guides in Metrology, 2008. Evaluation of measurement data - Guide to the expression of uncertainty in measurement (JCGM 100:2008).

Khanna, S., Kedare, S.B., Singh, S., 2013. Analytical expression for circumferential and axial distribution of absorbed flux on a bent absorber tube of solar parabolic trough concentrator. Solar Energy 92, 26-40.

Khanna, S., Singh, S., Kedare, S.B., 2015. Explicit expressions for temperature distribution and deflection in absorber tube of solar parabolic trough concentrator. Solar Energy 114, 289-302.

Khanna, S., Singh, S., Kedare, S.B., 2014. Effect of Angle of Incidence of Sun Rays on the Bending of Absorber Tube of Solar Parabolic Trough Concentrator. Energy Procedia 48, 123-129.

Lüpfert, E., Riffelmann, K., Price, H., Burkholder, F., Moss, T., 2008. Experimental Analysis of Overall Thermal Properties of Parabolic Trough Receivers. Journal of Solar Energy Engineering 130, 021007-021007.

Parretta, A., Antonini, A., Armani, M., Nenna, G., Flaminio, G., Pellegrino, M., 2007. Double-cavity radiometer for high-flux density solar radiation measurements. Appl. Opt. 46, 2166-2179.

Pérez-Rábago, C.A., Marcos, M.J., Romero, M., Estrada, C.A., 2006. Heat transfer in a conical cavity calorimeter for measuring thermal power of a point focus concentrator. Solar Energy 80, 1434-1442.

Riffelmann, K., Neumann, A., Ulmer, S., 2006. Performance enhancement of parabolic trough collectors by solar flux measurement in the focal region. Solar Energy 80, 1303-1313.

Röger, M., Herrmann, P., Ulmer, S., Ebert, M., Prahl, C., Göhring, F., 2014. Techniques to Measure Solar Flux Density Distribution on Large-Scale Receivers. Journal of Solar Energy Engineering 136, 031013-031013.

Schiricke, B., Pitz-Paal, R., Lüpfert, E., Pottler, K., Pfänder, M., Riffelmann, K., Neumann, A., 2009. Experimental Verification of Optical Modeling of Parabolic Trough Collectors by Flux Measurement. Journal of Solar Energy Engineering 131, 011004-011004.

Song, X., Huan, K., Dong, W., Wang, J., Zang, Y., Shi, X., 2014. Research on infrared radiation characteristics of Pyromark 1200 high-temperature coating. Proceedings of SPIE - the International Society for Optical Engineering, 9300, 93001S-1.